ISSN 1064-2269, Journal of Communications Technology and Electronics, 2013, Vol. 58, No. 2, pp. 101–109. © Pleiades Publishing, Inc., 2013.
Original Russian Text © A.P. Anyutin, 2013, published in Radiotekhnika i Elektronika, 2013, Vol. 58, No. 2, pp. 117–126.

ELECTRODYNAMICS AND WAVE PROPAGATION

Diffraction of Plane and Cylindrical Waves by a Cylindrical Metamaterial Shell with a Negative Refractive Index

A. P. Anyutin

Russian New University, ul. Radio 22, Moscow, 105005 Russia

e-mail: anioutine@mail.ru

Received June 29, 2012

Abstract—The problems of scattering of plane and cylindrical waves by a cylindrical metamaterial shell are solved rigorously. The influence of the geometric dimension of the shell, the value of the negative refractive index of the metamaterial medium, and the location of the cylindrical wave source on the near (far) field structure is investigated. It is shown that, in the quasi-opticl region, a caustic with one cusp is formed inside an electrically thick shell and whispering-gallery waves or standing waves are formed in between the facets of an electrically thin shell. It is found that, in the resonance region, reactive (surface) fields with substantial amplitudes are observed near the boundaries of a thin shell.

DOI: 10.1134/S1064226913020010

INTRODUCTION

At present, investigation of problems of diffraction of electromagnetic waves by dielectric bodies with a permittivity and a permeability that are simultaneously negative, ε_r and μ_r, is of substantial interest. The aforementioned constitutive parameters characterize a medium that is conventionally called a metamaterial. In particular, the problem of scattering of a plane wave or a cylindrical wave by a metamaterial shell of a finite thickness is interesting from both the practical and theoretical viewpoints, because its solution can contribute to the solution of the problem of masking (or providing for the invisibility effect, i.e., creating an invisibility cloak).

Note that the first theoretical study devoted to investigation of the interaction of plane and cylindrical waves with a plate made from such a medium was published in 1967 [1] and the first study reporting an experimentally created medium with a negative refractive index was published in 2000 [2]. In [2], such a medium was cal1ed a metamaterial and the effects predicted by Veselago in [1] were experimentally verified. Note that, in the modern scientific literature, the term *metamaterial* is used for any artificial media (although examples of such media—metal-dielectric materials—have been known since the middle of the twentieth century [3]).

By the present time, numerous studies devoted to theoretical and experimental investigations of various aspects of the problem of interaction of electromagnetic (or acoustic) waves with metamaterials have been published (see [4–12] and the references cited therein), and their number permanently increases. As a rule, theoretical studies are based on the application of various asymptotic methods, such as the geometric optics (GO) method and its various modifications or the Kirchhoff approximation [13]. The number of studies presenting rigorous numerical solutions to the corresponding problems is comparatively small (see [4] and the references cited therein).

It this study, we present a rigorous numerical solution to the 2D problem of scattering of a plane wave and a cylindrical wave by a cylindrical metamaterial shell whose maximal dimension substantially exceeds the wavelength. In contrast to study [5], we report results of rigorous calculation of the field distribution inside the scatterer and in its neighborhood (i.e., the structure of the near field).

1. FORMULATION OF THE PROBLEM AND DISCUSSION OF RESULTS

Consider the 2D problem of scattering of cylindrical wave $U_0(r, \varphi)$,

$$U_0(r,\varphi) = H_0^{(2)}\left(k\sqrt{r^2 + R_0^2 - 2rR_0\cos(\varphi - \varphi_0)}\right) \quad (1)$$

by a cylindrical shell (Fig. 1) with contours $\rho_{1,2}(\varphi)$ described by the equations

$$\begin{aligned} \rho_1(\varphi) &= a1; \\ \rho_2(\varphi) &= a2; \quad a1 > a2. \end{aligned} \quad (2)$$

In addition, it is assumed that the shell's medium in the region $a2 \le r \le a1$ has relative permittivity $\varepsilon_r < 0$ and relative permeability $\mu_r < 0$, i.e., is a metamaterial with the negative refractive index $n_1 = -\sqrt{|\varepsilon_r||\mu_r|} - i\nu$, where quantity ν characterizes the medium loss, and

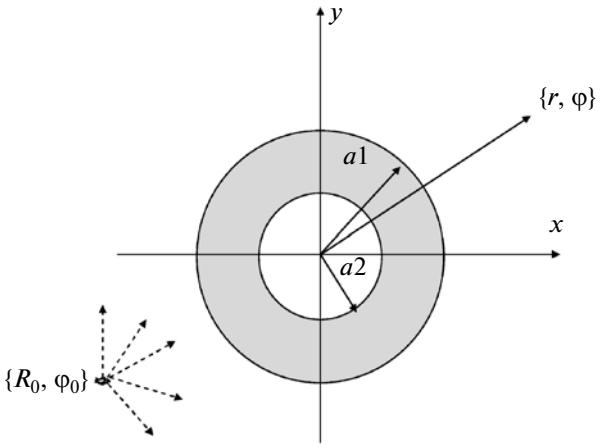

Fig. 1. Geometry of the problem. Dashed arrows denote GO rays.

k is the wave number in free space. In the interior ($r < a2$) and exterior ($r > a1$) of the shell, we have free space (vacuum) with the relative permittivity $\varepsilon_0 = 1$ and the relative permeability $\mu_0 = 1$.

Expressions (1) and (2) contain the following quantities: cylindrical spatial coordinates $\{r, \varphi\}$ of the observation point, cylindrical spatial coordinates $\{R_0, \varphi_0\}$ of the point of wave source Q, zero-order Hankel function of the second kind $H_0^{(2)}(\bullet)$, and parameters $a1$ and $a2$ characterizing the radii of the shell (the radii of the rings).

Total field $U(r, \varphi)$ beyond the shell can be represented as the superposition of incident wave field (1) and scattered field $U_1(r, \varphi)$

$$U(r,\varphi) = H_0^{(2)}\left(k\sqrt{r^2 + R_0^2 - 2rR_0\cos(\varphi - \varphi_0)}\right) + U_1(r,\varphi). \quad (3)$$

We denote the fields in the metamaterial and inside the shell $U_2(r, \varphi)$ and $U_3(r, \varphi)$, respectively.

As is known, fields $U(r, \varphi)$, $U_2(r, \varphi)$ and $U_3(r, \varphi)$ satisfy the corresponding Helmholtz equations in the exterior and interior of the shell and the corresponding boundary conditions on contours $\rho_1(\varphi)$ and $\rho_2(\varphi)$ of the shell. To solve numerically this boundary value problem, we apply the modified method of discrete sources (MMDS) [13–14], which enables us to obtain a solution with a controlled accuracy. In this method, fields $U_1(r, \varphi)$, $U_2(r, \varphi)$, and $U_3(r, \varphi)$ are represented as a superposition of the fields produced by auxiliary cylindrical wave sources located on auxiliary contours $\rho_{\Sigma 11}(\varphi)$, $\rho_{\Sigma 12}(\varphi)$, $\rho_{\Sigma 21}(\varphi)$, and $\rho_{\Sigma 22}(\varphi)$ inside and beyond contours $\rho_1(\varphi)$ and $\rho_2(\varphi)$. This representation automatically satisfies the Helmholtz equations and the Sommerfeld condition.

In the MMDS, the amplitude coefficients for the fields of auxiliary cylindrical wave sources are found from the boundary conditions fulfilled at N points of each of contours $\rho_1(\varphi)$ and $\rho_2(\varphi)$.

The accuracy of the solution to the problem is controlled through calculating the discrepancy of the boundary conditions at the centers of the intervals between the points where the boundary conditions are fulfilled exactly. At the aforementioned centers of intervals, the boundary conditions are satisfied with the worst accuracy [15]. The MMDS and the technique of its application to a number of problems with a similar configuration of a scatterer's contour are described in detail in [14, 15]. Therefore, we will not discuss the peculiarities of the MMDS application in the case under consideration and only note that the scattering patterns presented below are calculated with the maximum discrepancy of the boundary conditions that does not exceed the quantity $\Delta < 10^{-3}$ for any point of the corresponding contours.

First, let us consider the problem of diffraction of a plane wave (i.e., the case when the coordinates of the cylindrical wave source are assumed to be $kR_0 = 700$ and $\varphi_0 = \pi$) by a cylindrical shell with the electric radii $\rho_1 = ka1 = 10\pi$ and $\rho_2 = ka2 = 8\pi$. Thus, the thickness $kd = ka1 - ka2$ of the shell is assumed to be $kd = 2\pi$, i.e., equal to the wavelength. Physically, this means that we deal with the case of the diffraction of a plane wave by a relatively thin shell whose overall dimension is $kD = 2ka1 \gg 1$. Let the medium of such a shell be a metamaterial characterized by the relative permittivity $\varepsilon_r = -1.0001$, the relative permeability $\mu_r = -1.0001$, and the loss $\nu = -0.0001$.

Figure 2 shows the calculated spatial distribution of the total field and the equal-amplitude lines for the total field. It is seen from the results presented in this figure that the field practically is not scattered in the direction opposite to the direction of the incident plane wave propagation. In the interior of the shell, where $kr \le ka2$, the field is nonzero and localizes near the shell's back inner section. The field amplitude increases on the lateral segments of the outer (ρ_1) and inner (ρ_2) boundaries of the shell's contours (on the illuminated sections of the shell), and the shadow region behind the shell is illuminated. The interference structure of the field exists in the region adjacent to the inner shadow part of the shell.

The normalized scattering pattern for this case is displayed in Fig. 3. It follows from the pattern that the amplitude of the scattered field approaches zero in the region of angles close to the value $\varphi = \pi$ (i.e., in the direction opposite to the direction of the incident wave).

Consider the influence of the thickness of the shell (ring) on the spatial distribution of the field amplitude.

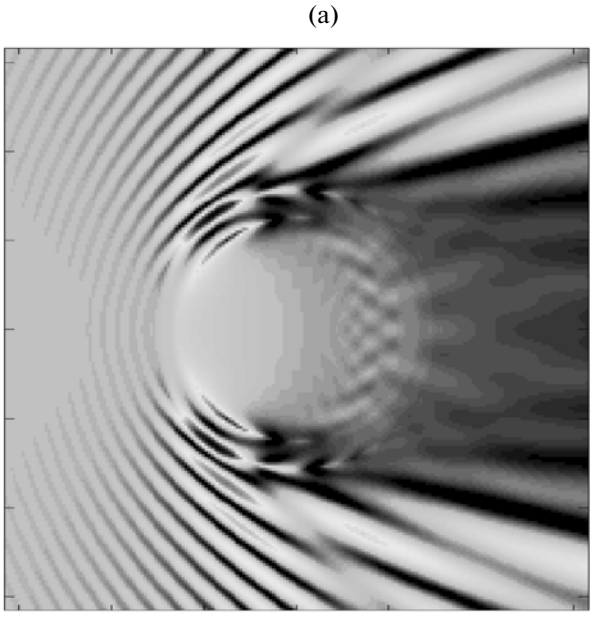

Fig. 2. Spatial distributions of the (a) total field amplitude and (b) equal-amplitude lines for the total field obtained for a plane wave incident on an electrically thin shell with $\varepsilon_r = -1.0001$ and $\mu_r = -1.0001$.

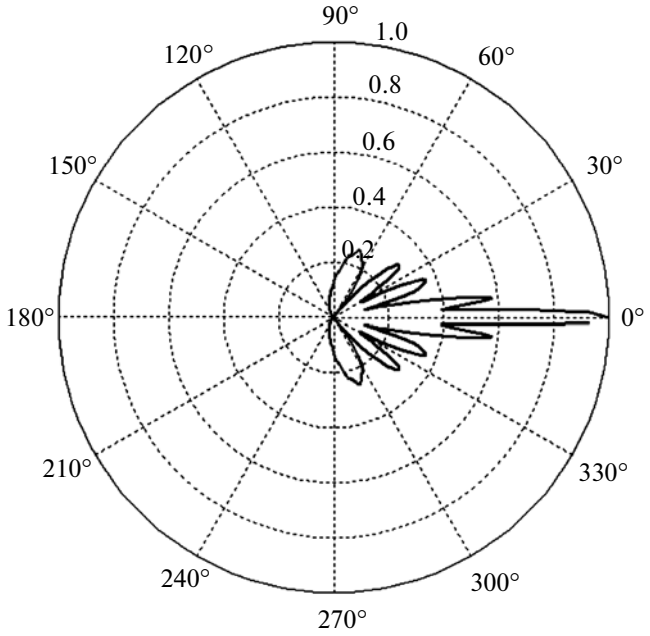

Fig. 3. Normalized scattering pattern obtained for a plane wave incident on an electrically thin shell with $\varepsilon_r = -1.0001$ and $\mu_r = -1.0001$. The numbers on the curves are the amplitude values.

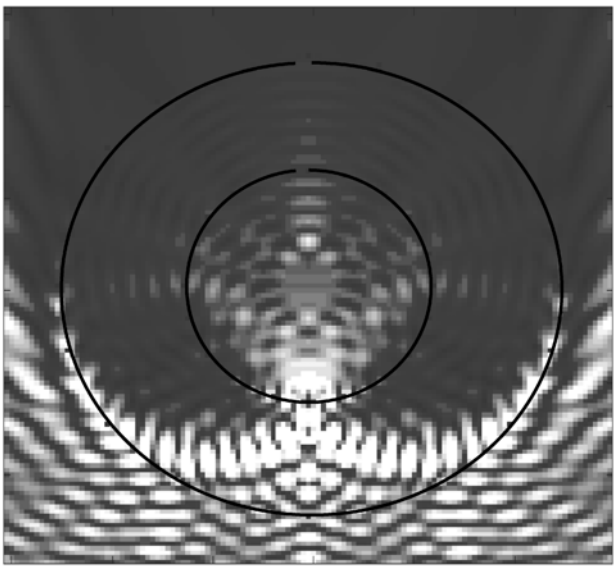

Fig. 4. Spatial distribution of the total field amplitude obtained for a plane wave incident on an electrically thick ring with $\varepsilon_r = -1.0001$ and $\mu_r = -1.0001$.

Let the geometry of the ring be characterized by the following values of parameters: $\rho_1 = ka1 = 40$ and $\rho_2 = ka2 = 20$ ($kd = ka1 - ka2 = 20 \gg 1$). The cylindrical wave source has the coordinates $kR_0 = 800$ and $\varphi_0 = -\pi/2$. The parameters of the metamaterial medium are the same as those indicated above. This means that we deal with the problem of diffraction of a plane wave by an electrically thick shell.

Figure 4 illustrates the spatial distribution of the field amplitude calculated for this case. It follows from this figure that the character of the spatial distribution of the field amplitude substantially differs from that observed in the case of an electrically thin ring considered above. Thus, in this case, we observe pronounced interference of the incident field and the field reflected by the ring, a circumstance that is not observed in the case of a thin ring. In addition, in the case of an elec-

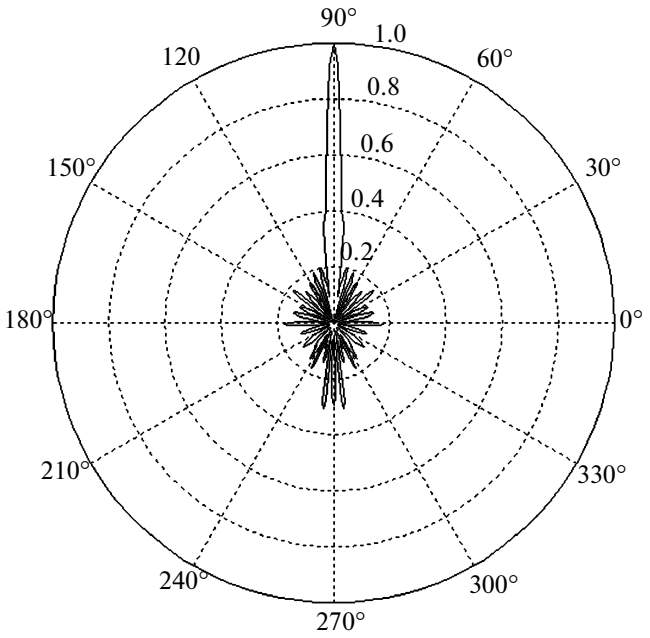

Fig. 5. Normalized scattering pattern obtained for a plane wave incident on an electrically thick ring with $\varepsilon_r = -1.0001$ and $\mu_r = -1.0001$. The numbers on the curves are the amplitude values.

trically thick ring, a symmetric caustic with one cusp is formed in the metamaterial-filled volume of the ring ($ka2 \le kr \le ka1$) [16] and a local focusing region is formed near boundary ρ_2. The field in the inner region of the ring (where $kr < ka2$) has a more intricate interference structure. Since the conditions for the GO applicability are fulfilled ($kD \gg 1$, $kd \gg 1$) for the electrically thick ring, we can attribute the field structure in the shell to focusing of GO rays refracted by the ring's outer boundary ρ_1 [16] and the existence of the field in the inner part to the refraction of GO rays by the ring's inner boundary ρ_2.

The normalized scattering pattern for this case is displayed in Fig. 5. We see that it qualitatively differs from the normalized scattering pattern for an electrically thin ring (see Fig. 3), because the field is scattered in the entire angle range $0 < \varphi < 2\pi$ (including the value $\varphi = -\pi/2$, which corresponds to the opposite direction).

Now, let us consider the influence of the curvature of the incident wave front. To this end, we place a cylindrical wave source near an electrically thick ring; i.e., we assume that the cylindrical wave source has the coordinates $kR_0 = 80$ and $\varphi_0 = -\pi$. The remaining parameters of the problem are the same as those indicated above. The structure of the spatial distribution of the total field amplitude in the exterior and interior of the ring is displayed in Fig. 6. The comparison of Figs. 6 and 4 shows that the peculiarities of the spatial distribution of the near field that are related with the formation of caustics and field focusing on the caustics are retained. The caustic in the inner region of the ring ($kr < ka2$) is more pronounced than in the case of a plane wave.

The normalized scattering pattern for this situation is displayed in Fig. 7. As is seen, it also substantially differs from the normalized scattering pattern for the case when a plane wave is incident on the ring (see Fig. 5).

It follows from the above results that, in the case of an electrically large ring ($kD \gg 1$) whose medium is a metamaterial with the parameters $\varepsilon_r = -1.0001$ and

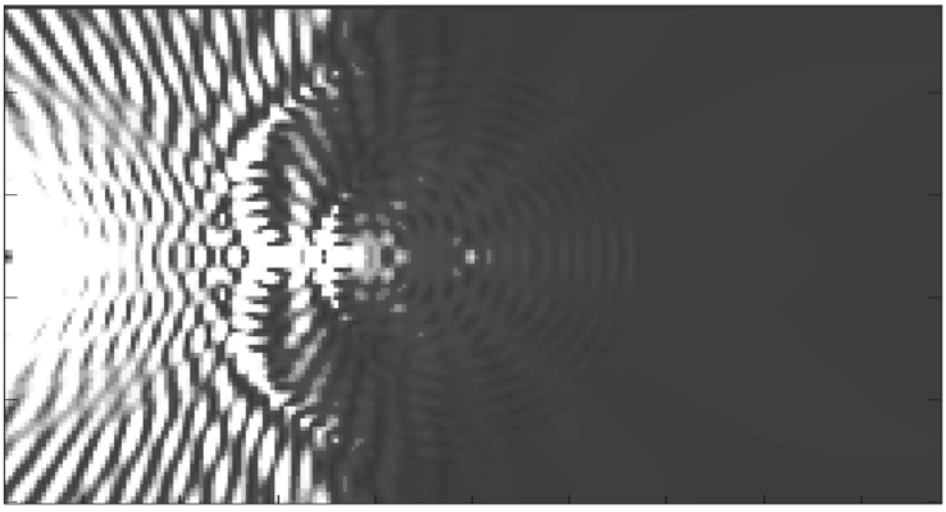

Fig. 6. Spatial distribution of the total field amplitude obtained for a cylindrical wave incident on an electrically thick ring with $\varepsilon_r = -1.0001$ and $\mu_r = -1.0001$.

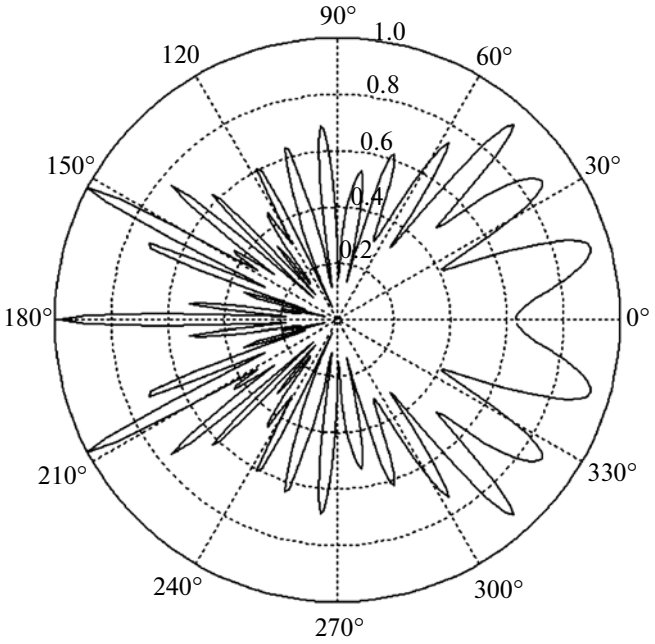

Fig. 7. Normalized scattering pattern obtained for a cylindrical wave incident on an electrically thick ring with $\varepsilon_r = -1.0001$ and $\mu_r = -1.0001$. The numbers on the curves are the amplitude values.

$\mu_r = -1.0001$, perfect field focusing (focusing into a single point) is observed for neither a plane incident wave nor a cylindrical incident wave. In the case of an electrically thick shell ($kd \gg 1$), the focusing process is accompanied by formation of a caustic with one cusp. In addition, we note that the field is scattered in all directions (though, in this case, the local reflection coefficient of the vacuum/metamaterial interface is zero in the GO approximation) and that the near field always has an interference structure.

Now, consider the case when the refractive index of the ring's metamaterial differs from unity and the ring's thickness is $kd = 2\pi$. Let the geometry of the problem and the metamaterial medium be characterized by the following parameters: $\varepsilon_r = -0.5$, $\mu_r = -0.5$, $ka1 = 10\pi$; $ka2 = 8\pi$, $kR_0 = 700$, and $\varphi_0 = \pi$. The spatial pattern of the distribution of the total field amplitude and the pattern of equal-amplitude lines for the total field are displayed in Figs. 8a and 8b, respectively. It is seen from the results presented in Fig. 8 that the field structure intrinsic to the field of a whispering-gallery wave is formed in the inner region of the ring ($kr \le ka2$) near the inner boundary $\rho_2 = ka2$. Surface waves exist on the boundary $\rho_2 = ka2$. In addition, in the illuminated region of the ring ($ka2 \le kr \le ka1$), the refracted field is focused on a caustic that has one cusp and branches located near the ring's boundary $\rho_2 = ka2$. Note that, in this case ($|n_1| < 1$), the focusing region (which is caustic branches) is located nearer to

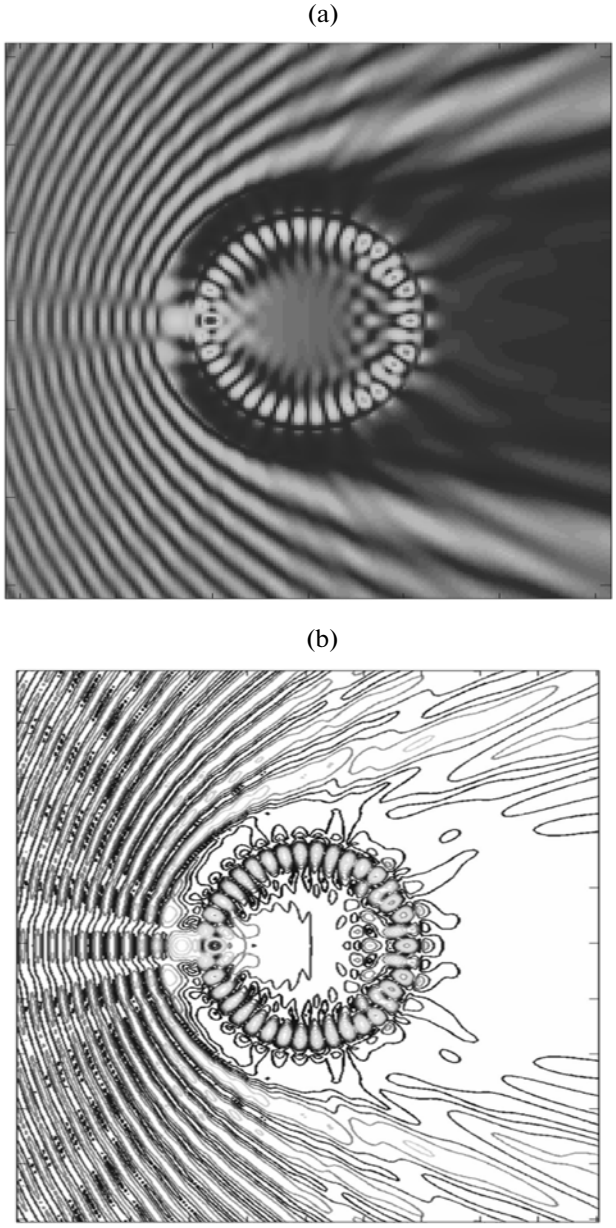

Fig. 8. Spatial distributions of the (a) total field amplitude and (b) equal-amplitude lines for the total field obtained for a plane wave incident on an electrically thin ring with $\varepsilon_r = -0.5$ and $\mu_r = -0.5$.

the boundary $\rho_2 = ka2$ than in the case $|n_1| = 1.0001$. In the remaining part of this region $ka2 \le kr \le ka1$, the field approaches zero.

From the standpoint of GO, this structure of the near field can be interpreted as follows. Some of the GO rays refracted by the outer boundary $\rho_1 = ka1$ of the ring are, at first, focused in the interior region $ka2 \le kr \le ka1$ of the ring (i.e., in the region located near the angle $\varphi \approx \pi$) and, then, are multiply refracted and reflected by the inner boundary $\rho_2 = ka2$. The GO

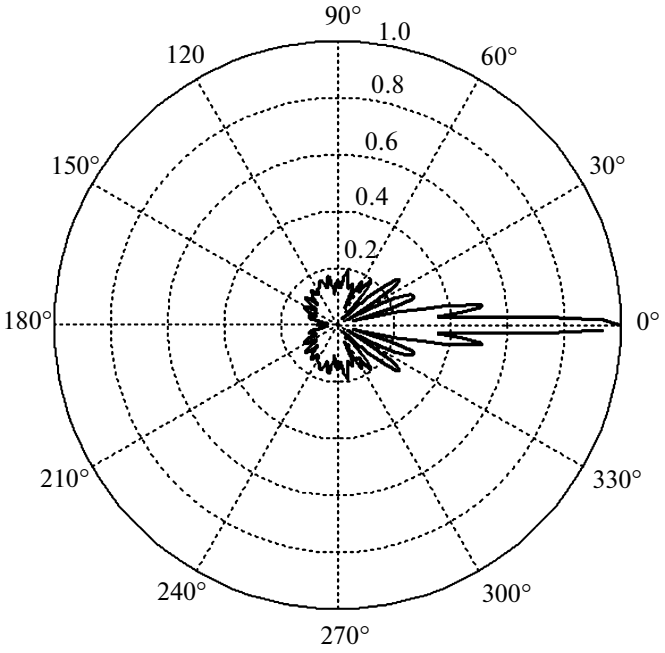

Fig. 9. Normalized scattering pattern obtained for a plane wave incident on an electrically thin ring with $\varepsilon_r = -0.5$ and $\mu_r = -0.5$. The numbers on the curves are the amplitude values.

rays refracted by this boundary and rereflected by the inner boundary $\rho_2 = ka2$ of the ring form a whispering-gallery wave. The angle of the incidence of the remaining GO rays on the outer contour $\rho_1 = ka1$ exceeds the angle of total reflection, a circumstance that causes the substantial attenuation of the field penetrating into the interior region $ka2 \le kr \le ka1$ of such a ring.

The normalized scattering pattern for this case is displayed in Fig. 9. It follows from this figure that the intensity of the backscattered field (observed in the region of angles $\varphi \approx \pi$) is close to zero.

In the case of an electrically thick ring ($ka1 = 10\pi$; $ka2 = 5\pi$), the aforementioned phenomena—focusing of GO rays in the region $ka2 \le kr \le ka1$ and surface waves on the boundary $\rho_2 = ka2$—are observed more distinctly. This circumstance is indicated by the calculated spatial structure of the total field amplitude and equal-amplitude lines of the total field that are displayed in Figs. 10a and 10b, respectively. Simultaneously, we can observe focusing of GO rays in the interior ($kr < ka2$) of the ring.

Similar phenomena also occur for a cylindrical incident wave (Fig. 11) whose source is located at the spatial point with the coordinates $kR_0 = 14\pi$ and $\varphi_0 = \pi$. The remaining parameters of the problem are retained.

Now, consider the case when the parameters of the ring's metamaterial are $\varepsilon_r = -2.0$ and $\mu_r = -2.0$; the outer and inner radii of the ring are $ka1 = 40$ and $ka2 = 30$, respectively; and the source of the cylindrical wave is located at the point with the coordinates $kR_0 = 80$ and $\varphi_0 = \pi$. The spatial distribution of the total field amplitude and equal-amplitude lines for the total field are displayed in Fig. 12.

(a)

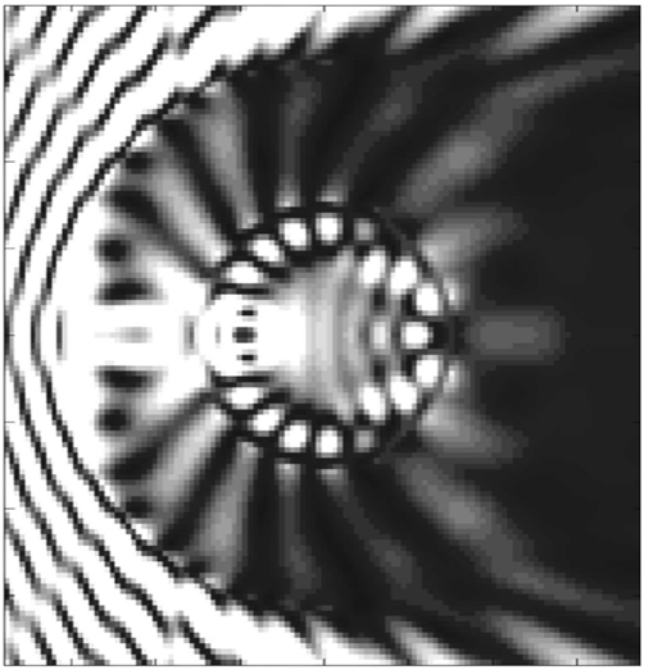

(b)

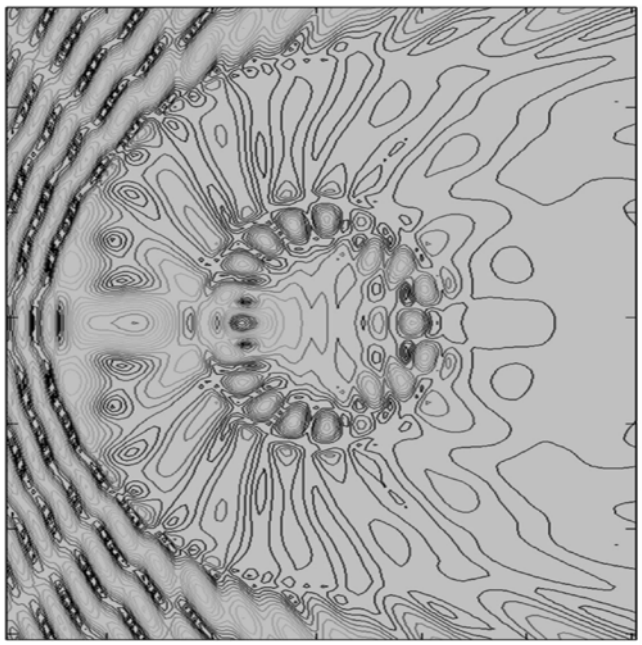

Fig. 10. Spatial distributions of the (a) total field amplitude and (b) equal-amplitude lines for the total field obtained for a plane wave incident on an electrically thick ring with $\varepsilon_r = -0.5$ and $\mu_r = -0.5$.

(a)

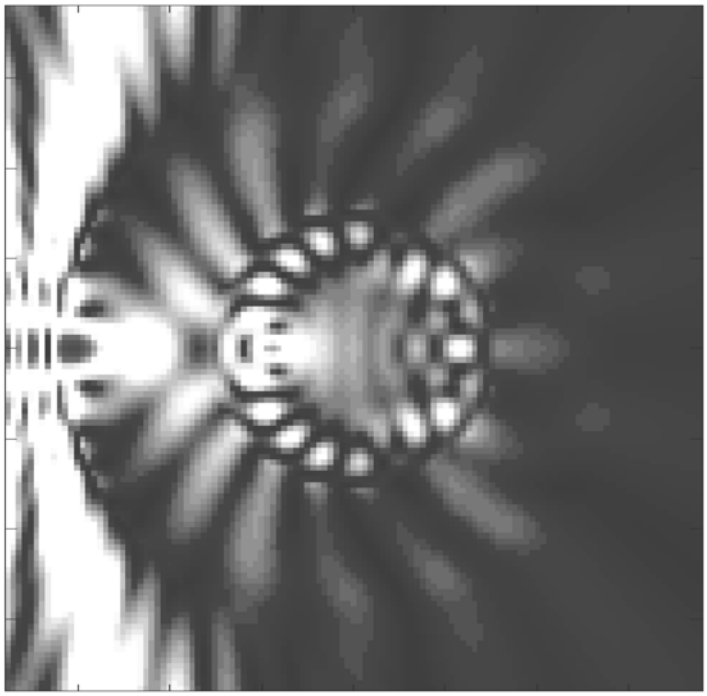

(b)

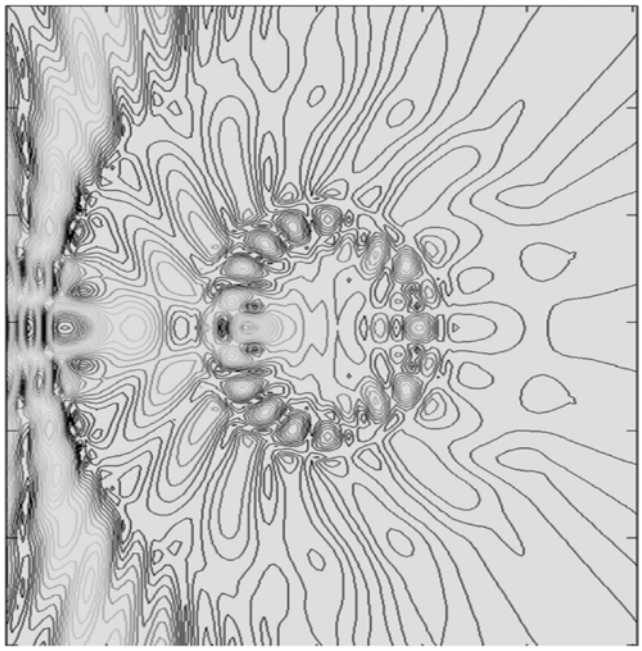

Fig. 11. Spatial distributions of the (a) total field amplitude and (b) equal-amplitude lines for the total field obtained for a cylindrical wave incident on an electrically thick ring with $\varepsilon_r = -0.5$ and $\mu_r = -0.5$.

In contrast to the case considered above, here, the field for $ka2 \le kr \le ka1$ has the structure intrinsic to the waveguide–interference mechanism of field propagation between two boundaries of the ring. Evidently, this situation is related with field rereflections between the shell's boundaries. Whispering-gallery waves are not formed in the interior region $kr < ka2$ of the ring.

For the case of an electrically thick ring when $ka1 = 40$; $ka2 = 20$, and the remaining parameters of the problem are retained, the spatial distribution of the

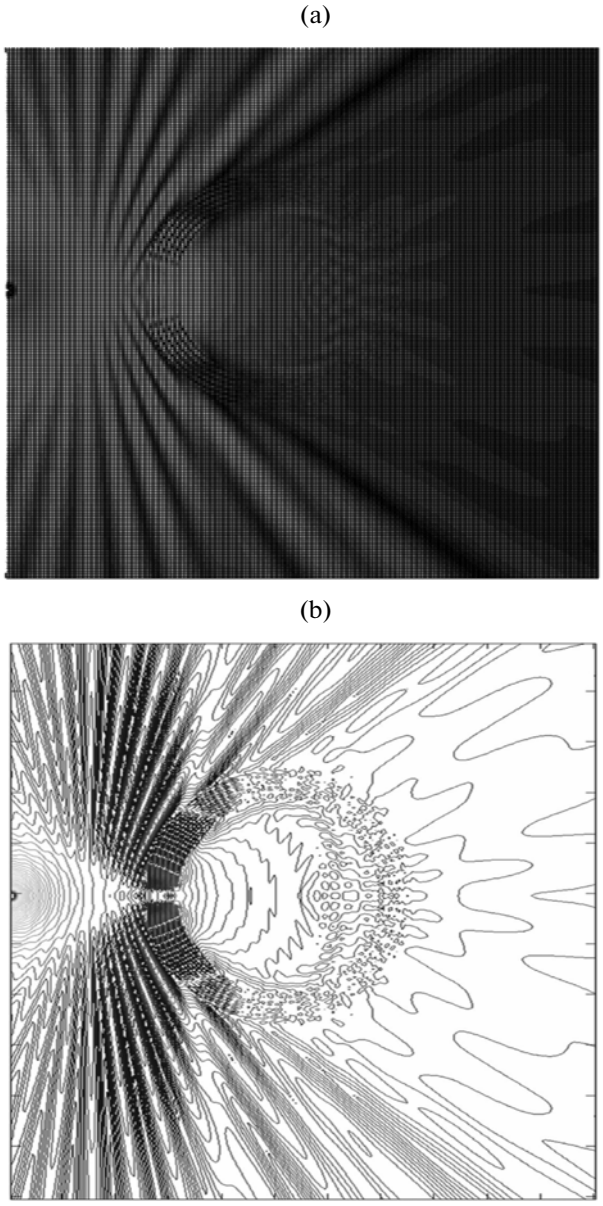

Fig. 12. Spatial distributions of the (a) total field amplitude and (b) equal-amplitude lines for the total field obtained for a cylindrical wave incident on an electrically thin ring with $\varepsilon_r = -2.0$ and $\mu_r = -2.0$.

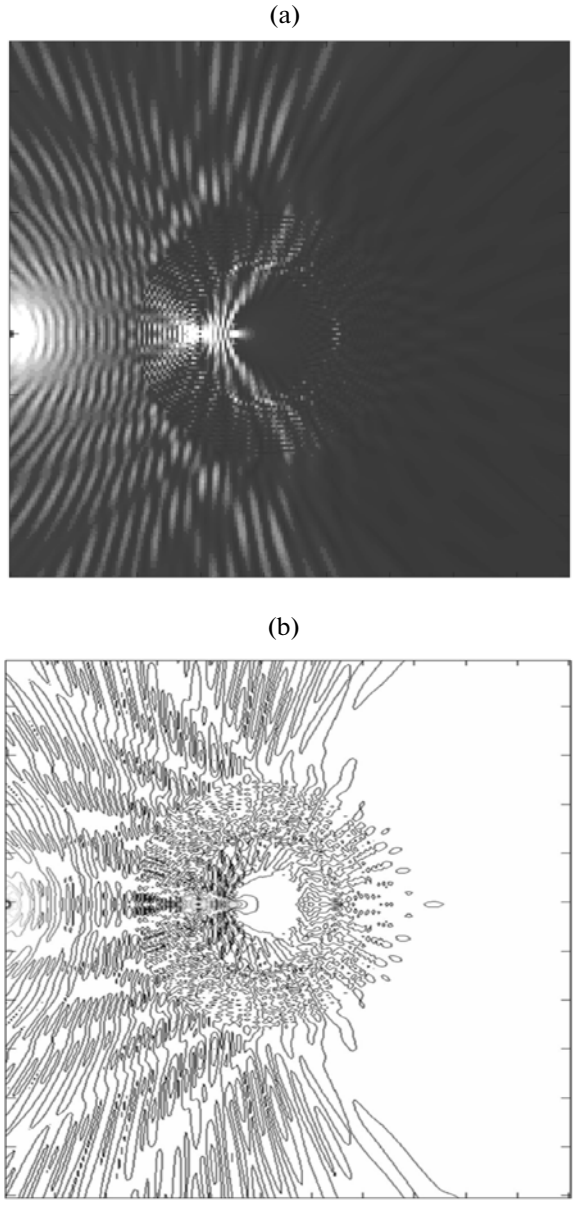

Fig. 13. Spatial distributions of the (a) total field amplitude and (b) equal-amplitude lines for the total field obtained for a cylindrical wave incident on an electrically thick ring with $\varepsilon_r = -2.0$ and $\mu_r = -2.0$.

total field amplitude and equal-amplitude lines for the total field are displayed in Figs. 13a and 13b, respectively. It is seen from the figure that the field inside the ring has an intricate interference structure that indicates the field focusing and interference effects in the ring's regions $kr < ka2$ and $ka2 \le kr \le ka1$.

The results presented above refer to the case when the maximum critical dimension of the ring satisfies the condition $kD = ka1 \gg 1$, i.e., the case of a quasi-optic region. In the case when $kD = ka1 \approx 2\pi$, i.e., in the quasi-resonance region, the diffraction of electromagnetic waves by such a ring differs from the diffraction in the case when $kD = ka1 \gg 1$. This conclusion can be drawn from the analysis of Fig. 14, which displays the spatial distribution of the total field amplitude and equal-amplitude lines for the total field calculated for the case when the dimensions of a thin ring $ka1 = 2\pi$ and $ka2 = ka1 - 1.5$ correspond to the quasi-resonance region and the cylindrical wave source has the coordinates $kR_0 = ka1 + 1$ and $\varphi_0 = \pi$. It follows from the figure that, in the process of diffraction of the cylindrical wave field by such a structure, surface waves

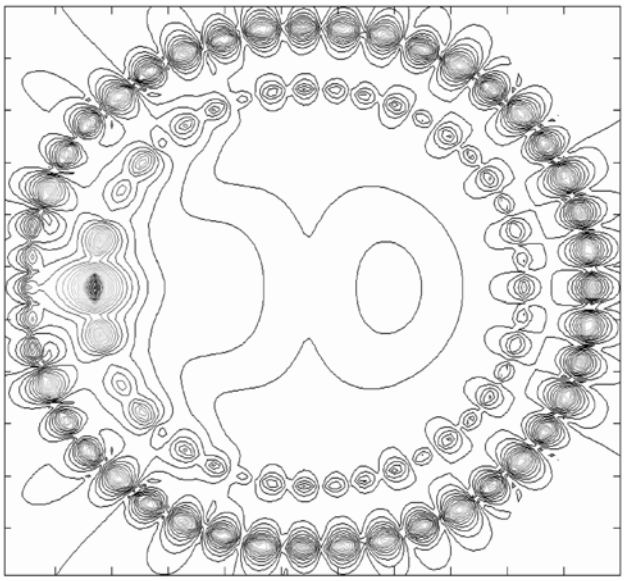

Fig. 14. Spatial distribution of equal-amplitude lines for a thin ring in the resonance region.

are formed on the inner ($r = a2$) and outer ($r = a1$) boundaries of the ring. The field in all of the remaining regions is unnoticeable against the background of the amplitude of surface waves.

ACKNOWLEDGMENTS

This study was supported by the Russian Foundation for Basic Research, project nos. 10-02-01103 and 12-02-00062-a.

REFERENCES

1. V. G. Veselago, Usp. Fiz. Nauk **92**, 517 (1967).
2. J. B. Pendry, Phys. Rev. Lett. **85**, 3966 (2000).
3. Ya. N. Fel'd and L. S. Benenson, *Antenna and Feeder Devices* (VVIA im. N. E. Zhukovskogo, Moscow, 1959), Part 2 [in Russian].
4. V. Veselago, L. Braginsky, V. Shklover, and C. J. Hafner, Comput. Theor. Nanosci. **2**, 1 (2006).
5. A. P. Anyutin, J. Radioelectron., No. 7 (2007). http://ire/cplire.ru
6. A. D. Shatrov, J. Commun. Technol. Electron. **52**, 842 (2007).
7. A. P. Anyutin, J. Commun. Technol. Electron. **53**, 387 (2008).
8. A. P. Anyutin, J. Commun. Technol. Electron. **53**, 1323 (2008).
9. A. B. Petrin, JETP **106**, 963 (2008).
10. A. P. Anyutin, J. Commun. Technol. Electron. **54**, 982 (2009).
11. V. P. Mal'tsev and A. D. Shatrov, J. Commun. Technol. Electron. **55**, 278 (2010).
12. A. P. Anyutin, J. Commun. Technol. Electron. **55**, 132 (2010).
13. A. S. Kryukovskii and D. S. Lukin, *Edge and Angular Catastrophes in Uniform Geometrical Theory of Diffraction* (MFTI, Moscow, 1999) [in Russian].
14. A. P. Anioutine, A. G. Kyurkchan and S. A. Minaev, J. Quant. Spectrosc. Radiat. Transf. **79**, 509 (2003).
15. A. G. Kyurkchan, S. A. Minaev, and A. L. Soloveichik, J. Commun. Technol. Electron. **46**, 615 (2001).
16. A. P. Anyutin, J. Commun. Technol. Electron. **56**, 1029 (2011).